

Temperature Simulation In The Furnace With Rotary Hearth, Using Taylor Series

Vlad Muresan, Mihail Abrudean

Department of Automation, Technical University of Cluj-Napoca
 Vlad.Muresan@aut.utcluj.ro, Mihai.Abrudean@aut.utcluj.ro

Abstract: This work presents a numerical simulation method associated with Taylor series of the control system of the temperature value in the furnace with rotary hearth.

Keywords: furnace with rotary hearth, analogue modelling, numerical simulation, equations with partial derivatives (EDP).

1. INTRODUCTION

The furnace with rotary hearth (CRV) is one of the basic aggregates in the technologic flow for manufacturing seamless pipes. Its purpose is to warm up the blocks of billets, previously cut at the required lengths, from the environment's temperature to the rolling temperature, leading the material from the elastic domain to the plastic one. The furnace is heated using methane gas.

The furnace is a CARUSEL one (with rotary hearth), working continuously in the technologic flow of the rolling line [1].

The furnace has five regulating temperature sectors, which have a total of 48 burners, a sector for preheating and a sector for loading-unloading. For the supply and evacuation of the blocks, the furnace has a loading machine and one for evacuation [2].

The methane gas supply is made through a pipe from the natural gas system that branches in two, a main one and a by pass one. The gas that exists from these two pipes is being sent to other five pipes, each of them supplying one of the 5 active sectors of the furnace. Sector 6 supplies from the pipe of sector 5. While working in service duty, sector 6 is thermally inactive.

The temperatures corresponding to each sector are being adjusted by adjusting the gas flow on the corresponding pipes. The temperature in each sector is measured using 2 thermocouples (for redundancy). The signal from the thermocouples exit is being sent to the flow controllers. Each controller (there is one for each of the 5 active sectors) is of PID type and controls the flow on the pipes operating some pneumatic actuators as valves situated on the five supply gas pipes.

The air supply is made by 3 ventilators. The obstruction mechanisms of ventilators air absorption are blocked from the start in order to protect the ventilators motors and then they are being started step by step. These three mechanisms are of multi-leaf type. The extra air supply is made in such a way that it respects the air / gas ratio of 9-10/1 in the furnace. The pressure in the furnace is being measured using some differential pressure cells in order to keep an overpressure comparing to the atmospheric pressure, of 2,5 mm H₂O. The burnt gases are evacuated through a pipe that gets into a heat

interchanger that has the role to pre heat the air needed for burning.

The methane gas gets from the supply gas system of the factory with a variable pressure of about 0.3-1 bar. The reduction units have the role to maintain the supply pressure of the furnace at a constant level, between 60 and 80 mbar with the possibility to adjust.

2. MODELING THE THERMAL PROCESSES FOR EACH SECTOR OF THE FURNACE USING PARTIAL DERIVATIVES EQUATIONS

Modeling the thermal systems in this case can be done considering the temperature variation between the furnace interior and exterior wall. In this way in the internal centre of the furnace we can measure the highest temperature and near the walls of the furnace we can measure the lowest temperature of that sector. The dependence of temperature on length can mathematically be expressed as an exponential function. This variation is due to the following three major factors [3]:

i) The burners are assembled in the walls of the furnace and the tops of the flames get close to the centers of the sectors. On the top of the flames the burning is complete and the temperature is higher than within their bodies or at their root.

ii) The temperature dissipations are due to the isolation of the furnace and to the fact that the temperature of the neighboring environment is the ambient temperature.

iii) The burnings are disposed in opposition and their flames meet in the centers of the sectors, the thermal effect being stronger.

The analogue model of the processes with the distributed parameters can be expressed using equations and systems of partial derivatives equations. Thus, besides the time variable (t), in the Cartesian space we introduce the independent variables (p), (q) and (r) in the model of processes.

The axes that determine the Cartesian space are 0p, 0q and 0r.

The five thermal systems corresponding to the active sectors of the furnace are modeled through equations with partial derivatives. All of them have the same structure (the equation

order and the number of independent variables) but have different coefficients.

To make it simpler we define the Cartesian variable (s):

$$s = s(p, q, r) = \pm\sqrt{p^2 + q^2 + r^2} \tag{1}$$

and

$$y = y(t, s). \tag{2}$$

Due to the turbulences from the inside of the furnace, due to the small height of work space and due to the control of temperature on each sector separately, it is not necessary to discuss the problem on directions (q) and (r). We also adopt the convention that variable (s) has got only positive values. In this way relation (1) becomes:

$$s = s(p,0,0) = \sqrt{p^2 + 0^2 + 0^2} = p \tag{3}$$

Introducing variable (s), the equation with partial derivatives that describes the process work (EDP II.2) becomes:

$$a_{00} \cdot y + a_{10} \cdot \frac{\partial y}{\partial t} + a_{01} \cdot \frac{\partial y}{\partial s} + a_{20} \cdot \frac{\partial^2 y}{\partial s^2} + a_{11} \cdot \frac{\partial^2 y}{\partial t \partial s} + a_{02} \cdot \frac{\partial^2 y}{\partial s^2} = j(t, s) \cdot u(t) \tag{4}$$

In relation (4) the coefficients are constant and the functions y (t,s) and φ₀₀ (t, s) respect Cauchy conditions of continuity.

If we consider:

$$x_{TS} = \frac{\partial^{T+S} y}{\partial t^T \partial s^S} \tag{5}$$

where T=0,1,2,....., and S=0,1,2,....., relation (4) can be written as:

$$a_{00} \cdot x_{00} + a_{10} \cdot x_{10} + a_{01} \cdot x_{01} + a_{20} \cdot x_{20} + a_{11} \cdot x_{11} + a_{02} \cdot x_{02} = j_{00} \cdot u_0 \tag{6}$$

For a higher generality and in order to have the possibility to introduce the model of heating the bills in the process, we worked with an equation (EDP II.2).

Due to the fact that the process has only a significant time constant (T₁), the time constant (T₂) has an insignificant value controlled through the very small value of the (I_T) parameter. (I_T) parameter is a coefficient that shows the proportion between the two time constants. The general approach from the first chapter works for all the five active sectors of the furnace with rotary hearth.

3. ANALOGUE MODELING OF THE AUTOMATIC CONTROL SYSTEMS

In order to have a furnace with rotary hearth that works in good conditions, more precisely for a good heating of the billets in the furnace, we need to control the temperature in each active sector of the furnace. The control rule that is going to be implemented is of PID type [4]. From now on we are going to present the general scheme of automatic control of the temperature in the sectors of the furnace. This scheme

can be applied to any of the five active sectors of the furnace with rotary hearth.

The general scheme of automatic control is presented in figure 1.

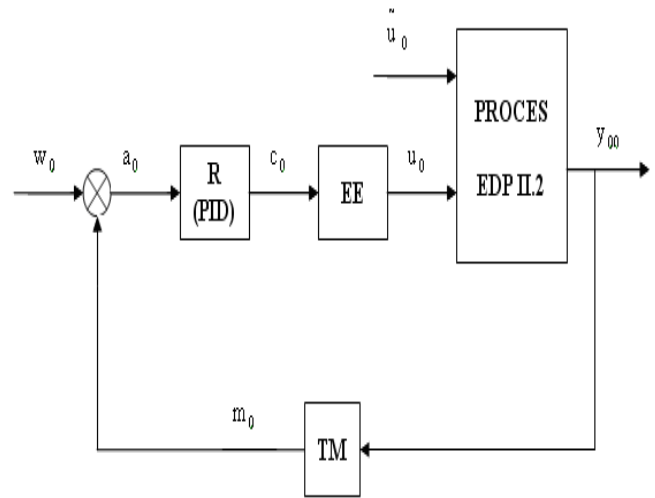


Fig. 1. General scheme of automatic control.

In figure 1 the significance of the notations is:

R - controller of PID type;

EE- actuator;

TM- transducer;

w₀ - reference signal;

m₀ - measure signal;

a₀ - error signal (a₀ = w₀ - m₀);

c₀ - control signal;

u₀ - execution signal represents the input of methane gas flow, after the actuation generated by the controller;

\tilde{u}_0 - disturbance signal (stretching the terminology, it can be considered the flow of methane gas that has to be subtracted from signal u₀, equivalent to the negative thermal effect generated by the introduction of billets in the furnace);

y₀₀ - output signal (sector temperature).

The thermal processes work, as shown in the previous chapter, is modeled using equations with partial derivatives of second order (EDP II.2) with two independent variables (time (t) and space variable (s)) in Cartesian coordinates.

The analogue modeling of the system presented in figure 1 starts from the following system of equations:

$$\text{Transducer: } \begin{cases} m_0 \\ m_1 = \frac{1}{T_T} \cdot (K_T \cdot y_{00} - m_0) \end{cases} \tag{7}$$

PID controller:

$$\left\{ \begin{array}{l} c_0 \\ c_1 = \frac{1}{T_R} \cdot [K_{PR} \cdot (w_0 - m_0) + K_{DR} \cdot (w_1 - m_1) - c_0] \\ c_2 = \frac{1}{T_R} \cdot [K_{PR} \cdot (w_1 - m_1) + K_{IR} \cdot (w_0 - m_0) + \\ + K_{DR} \cdot (w_2 - m_2) - c_1] \end{array} \right. \quad (8)$$

Actuator:

$$\left\{ \begin{array}{l} u_0 \\ u_1 = \frac{1}{T_{EE}} \cdot (K_{EE} \cdot c_0 - u_0) \end{array} \right. \quad (9)$$

Process EDP II.2:

$$\left\{ \begin{array}{l} y_{00} \\ y_{10} \\ y_{20} = \frac{1}{a_{20}} \cdot [j_{00} \cdot u_0 - (a_{00} \cdot y_{00} + a_{10} \cdot y_{10} + \\ + a_{01} \cdot y_{01} + a_{11} \cdot y_{11} + a_{02} \cdot y_{02})] \end{array} \right. \quad (10)$$

Only a subscript attached to the elements from relations (7)...(10) signifies the derivate order of those elements related to the independent variable (t). In the previous relations, the following symbols have also been used: K_T - the proportionality constant of the transducer, T_T - time constant of the transducer, K_{PR} - proportionality constant of the controller, K_{IR} - integration constant of the controller, K_{DR} - derivation constant of the controller, T_R - inertial time constant of the controller, K_{EE} - proportionality constant of the actuator and T_{EE} - time constant of the actuator.

The relations (7), (8), (9) and (10) give the elements of the state vector \mathbf{x} that in transposed form is being presented in relation (11):

$$\mathbf{x}^T = \begin{bmatrix} m_0 & m_1 & c_0 & c_1 & u_{s0} & u_{s1} & y_{00} & y_{10} \end{bmatrix} \quad (11)$$

We can notice that the vector \mathbf{x} has got 8 elements, so it has the dimension (8·1) ($\mathbf{x}(8 \cdot 1)$). Also $m_0, m_1, c_0, c_1, u_0, u_1$ are functions that depend only on the time variable (t), and y_{00} and y_{10} are functions that depend on time (t) and on the independent variable length (s).

When we consider the values $M=8$ and $N=20$, definitive for the dimension of matrix M_{dpx} (the matrix of partial derivatives of the state vector), it is presented in relation (12).

The matrices and vectors that occur in relation (12) are: [5]

- the state vector \mathbf{x} of the whole system with dimension (8·1) ($\mathbf{x}(8 \cdot 1)$);
- the vector of partial derivatives related to time (t) of the state vector \mathbf{x}_T with dimensions (20·1) ($\mathbf{x}_T(20 \cdot 1)$);
- the matrix of partial derivatives related to independent variable (s) of the state vector \mathbf{x}_S with dimension (8·8) ($\mathbf{x}_S(8 \cdot 8)$);
- the matrix of partial derivatives related to time (t) and to the independent variable (s) of the state vector \mathbf{x}_{TS} with the dimension (20·8) ($\mathbf{x}_{TS}(20 \cdot 8)$).

Thus it results that the matrix M_{dpx} has the dimension (28·9) ($M_{dpx}(28 \cdot 9)$).

In relation (12) the lines that correspond to the state variables $m_0(t), c_0(t), u_0(t)$ and to their derivatives related to time (t) contain only elements equal to 0, because when deriving functions that depend only on time (t) related to the independent variable length (s), the resulted values are 0.

Due to the inertia of the components of the automatic control system, for the initial conditions ($t=t_0=0$): $m_{0,CI}=0, c_{0,CI}=0, u_{0,CI}=0$. The other elements of the state vector that correspond to the initial conditions (CI) are:

	1 ← M=8										
	m_0	0	0	0	0	0	0	0	n=8		
	m_1	0	0	0	0	0	0	0			
	c_0	0	0	0	0	0	0	0			
	c_1	0	0	0	0	0	0	0			
	u_0	0	0	0	0	0	0	0			
	u_1	0	0	0	0	0	0	0			
	y_{00}	y_{01}	y_{02}	y_{03}	y_{04}	y_{05}	y_{06}	y_{07}		y_{08}	
	y_{10}	y_{11}	y_{12}	y_{13}	y_{14}	y_{15}	y_{16}	y_{17}		y_{18}	
$M_{dpx} =$	x	x_s	↑ n=20	m_2	0	0	0	0	0	0	0
	x_T	x_{TS}		c_2	0	0	0	0	0	0	0
			u_2	0	0	0	0	0	0	0	
			y_{20}	y_{21}	y_{22}	y_{23}	y_{24}	y_{25}	y_{26}	y_{27}	y_{28}
			m_3	0	0	0	0	0	0	0	0
			c_3	0	0	0	0	0	0	0	0
			u_3	0	0	0	0	0	0	0	0
			y_{30}	y_{31}	y_{32}	y_{33}	y_{34}	y_{35}	y_{36}	y_{37}	y_{38}
			m_4	0	0	0	0	0	0	0	0
			c_4	0	0	0	0	0	0	0	0
			u_4	0	0	0	0	0	0	0	0
			y_{40}	y_{41}	y_{42}	y_{43}	y_{44}	y_{45}	y_{46}	y_{47}	y_{48}
			m_5	0	0	0	0	0	0	0	0
			c_5	0	0	0	0	0	0	0	0
			u_5	0	0	0	0	0	0	0	0
			y_{50}	y_{51}	y_{52}	y_{53}	y_{54}	y_{55}	y_{56}	y_{57}	y_{58}
			m_6	0	0	0	0	0	0	0	0
			c_6	0	0	0	0	0	0	0	0
			u_6	0	0	0	0	0	0	0	0
			y_{60}	y_{61}	y_{62}	y_{63}	y_{64}	y_{65}	y_{66}	y_{67}	y_{68}

(12)

$$m_{1,CI} = \frac{1}{T_T} \cdot (K_T \cdot y_{00,CI} - m_{0,CI}). \quad (13)$$

$$c_{1,CI} = \frac{1}{T_R} \cdot [K_{PR} \cdot (w_{0,CI} - m_{0,CI}) + K_{DR} \cdot (w_{1,CI} - m_{1,CI}) - c_{0,CI}] \quad (14)$$

$$u_{1,CI} = \frac{1}{T_{EE}} \cdot (K_{EE} \cdot c_{0,CI} - u_{0,CI}). \quad (15)$$

To calculate the elements $y_{00,CI}$, $y_{10,CI}$, $(\frac{\partial^r y_{00}}{\partial s^r})_{CI}$ and $(\frac{\partial^r y_{10}}{\partial s^r})_{CI}$, where $r \in \{1,2,\dots,M\}$, we use the analytical solution. Thus, after computing we get: $y_{00,CI}=0$,

$$y_{10,CI}=0, y_{0r,CI}=0 \quad \text{and} \quad y_{1r,CI} = (\frac{\partial^r y_{10}}{\partial s^r})_{CI}=0, \quad \text{where} \\ r \in \{1,2,\dots,M\}.$$

In the previous relations all the elements of the vector $\mathbf{x}_{CI} = \mathbf{x}(t_0, s)$ have been calculated and of the matrix $\mathbf{x}_{S,CI} = \mathbf{x}_S(t_0, s)$.

The pivot elements are:

$$m_2 = \frac{1}{T_T} \cdot (K_T \cdot y_{10} - m_1). \quad (16)$$

$$c_2 = \frac{1}{T_R} \cdot [K_{PR} \cdot (w_1 - m_1) + K_{IR} \cdot (w_0 - m_0) + K_{DR} \cdot (w_2 - m_2) - c_1] \quad (17)$$

$$u_2 = \frac{1}{T_{EE}} \cdot (K_{EE} \cdot c_1 - u_1). \quad (18)$$

$$y_{20} = \frac{1}{a_{20}} \cdot [j_{00} \cdot u_0 - (a_{00} \cdot y_{00} + a_{10} \cdot y_{10} + a_{01} \cdot y_{01} + a_{11} \cdot y_{11} + a_{02} \cdot y_{02})] \quad (19)$$

Using the previous results and replacing them in the relations (16), (17), (18) and (19), we get the pivot elements for the initial conditions (CI):

$$m_{2,CI} = \frac{1}{T_T} \cdot (K_T \cdot y_{10,CI} - m_{1,CI}). \quad (20)$$

$$c_{2,CI} = \frac{1}{T_R} \cdot [K_{PR} \cdot (w_{1,CI} - m_{1,CI}) + K_{IR} \cdot (w_{0,CI} - m_{0,CI}) + K_{DR} \cdot (w_{2,CI} - m_{2,CI}) - c_{1,CI}] \quad (21)$$

$$u_{2,CI} = \frac{1}{T_{EE}} \cdot (K_{EE} \cdot c_{1,CI} - u_{1,CI}). \quad (22)$$

$$y_{20,CI} = \frac{1}{a_{20}} \cdot [j_{00} \cdot u_0 - (a_{00} \cdot y_{00} + a_{10} \cdot y_{10} + a_{01} \cdot y_{01} + a_{11} \cdot y_{11} + a_{02} \cdot y_{02})]_{CI} \quad (23)$$

In the relation (23) $j_{00,CI} = j_{00}(t, s)_{CI}$.

The vector $\mathbf{x}_{T,CI}$ is obtained from the state vector, if we derive successively its elements in relation to the independent variable time (t). The first element of the vector (\mathbf{x}_T) is the pivot element, meaning (x_{n0}). There is also the condition that $N \geq n$.

The matrix $\mathbf{x}_{TS,CI}$ is obtained from the elements of the matrix (\mathbf{x}_S) through their successive derivation in relation to the independent variable time (t), starting from the left side to the right side of a line and finishing the calculation for a line, before passing to the calculation of the line below. The elements that result represent partial derivatives in relation to time (t) of the elements of matrix (\mathbf{x}_S), and $T \in \{n, n+1, \dots, n-1+N\}$.

After doing these calculations we can make the matrix (M_{dpx}) for the initial conditions ($(M_{dpx})_{CI}$) that correspond to the start sequence (k-1).

Using this version we can highlight the evolutions in time of the variables u(t), c(t), m(t) and y(t).

4. NUMERICAL SIMULATION OF THE AUTOMATIC CONTROL CIRCUITS

In order to advance from sequence (k-1) to sequence (k) we need to use the Taylor series. According to the method that has been presented in [6], in order to calculate the elements of the state vector (\mathbf{x}) at moment (k) we should apply the formula:

$$x_{t0,k} \cong x_{t0,k-1} + \sum_{T=t+1}^{N+n-1} \frac{\Delta t^{T-t}}{(T-t)!} \cdot x_{T0,k-1}, \quad (24)$$

and in order to calculate the elements of the matrix with partial derivatives of the state vector, (\mathbf{x}_S) at the moment (k) we should apply the formula:

$$x_{tj,k} \cong x_{tj,k-1} + \sum_{T=t+1}^{N+n-1} \frac{\Delta t^{T-t}}{(T-t)!} \cdot x_{Tj,k-1}, \quad (25)$$

where $t \in \{0,1,\dots,n-1\}$, $j \in \{1,2,3,\dots,M\}$, $n=8$, $N=20$ și $M=8$. The formulas presented above are valid if the integration is being done in relation to time (t).

Due to the fact that in relation (12) the maximum derivation order in relation to time (t) of function m(t) is 6 (m_6), of function c(t) is 6 (c_6), of function u(t) is 6 (u_6), and of function y(t) is 6 (y_{6i} , $i \in \{1,2,\dots,M\}$, and $M=8$), the terms

with higher derivation orders are not complete We can notice that $N+n-1=20+8-1=27$.

The elements $(m_{0k}), (m_{1k}), (c_{0k}), (c_{1k}), (u_{0k}), (u_{1k})$ $(y_{00,k})$ and $(y_{10,k})$ of the state vector (\mathbf{x}) are given by the relations:

$$m_{t,k} \cong m_{t,k-1} + \sum_{T=t+1}^6 \frac{\Delta t^{T-t}}{(T-t)!} \cdot m_{T,k-1}, \quad (26)$$

$$c_{t,k} \cong c_{t,k-1} + \sum_{T=t+1}^6 \frac{\Delta t^{T-t}}{(T-t)!} \cdot c_{T,k-1}, \quad (27)$$

$$u_{t,k} \cong u_{t,k-1} + \sum_{T=t+1}^6 \frac{\Delta t^{T-t}}{(T-t)!} \cdot u_{T,k-1}, \quad (28)$$

$$y_{t0,k} \cong y_{t0,k-1} + \sum_{T=t+1}^6 \frac{\Delta t^{T-t}}{(T-t)!} \cdot y_{T0,k-1}. \quad (29)$$

In the relations (26), (27), (28) și (29) $t \in \{0,1\}$.

The functions $(m_0), (m_1), (c_0), (c_1), (u_0)$ and (u_1) do not depend on length (s), so the lines that correspond to them from the matrix (x_s) contain elements equal to 0. Using the Taylor series we can approximate the elements (y_{tj}) , for $t \in \{0,1\}, j \in \{1,2,\dots,M\}$, and $M=8$, in the following way:

$$y_{tj,k} \cong y_{tj,k-1} + \sum_{T=t+1}^6 \frac{\Delta t^{T-t}}{(T-t)!} \cdot y_{Tj,k-1}. \quad (30)$$

After compensating the pair of relations (30) and (31), it results:

$$y_{tj,k} \cong y_{tj,k-1} + \sum_{T=t+1}^6 \frac{\Delta t^{T-t}}{(T-t)!} \cdot y_{Tj,k-1}. \quad (31)$$

Where in both $t \in \{0,1\}, j \in \{0,1,2,\dots,8\}$.

Using the calculated values we get the elements of the vectors (\mathbf{x}_T) and (\mathbf{x}_{TS}) as per the algorithm presented in the previous chapter.

In both versions the numerical simulation is finished when $t \geq t_f$ (final simulation time).

In all the relations from this subchapter we considered that the integration step (Δt) has a value that is small enough, so that the numerical integration is being done correctly. The value of (Δt) is in general smaller than the 10th part of the smaller time constant from the system. This value is chosen according to the specific of the application.

5. THE SIMULATION RESULTS

The simulation application has been developed in MATLAB environment [7].

After simulation we have compared the response that resulted through numerical integration and the analytical response of the system. We calculate the error and represent it on a graph (the relative error cumulated in percents). The formula of the error cumulated in percents is presented in relation (32):

$$\text{ercpy} = 100 \cdot \frac{\sum_{i=1}^{i_f} |y_{Ni} - y_{Ai}|}{\sum_{i=1}^{i_f} |y_{Ai}|}. \quad (32)$$

In the relation (32): i represents the integration sequence; i_f represents the integration final sequence; y_{Ni} represents the value of the system response resulted through numerical integration, that corresponds to sequence i ; y_{Ai} represents the value of the system analytical response that corresponds to sequence i . The value that resulted after calculating the error is in percents.

In the first sector of the furnace, the automatic control system has the role to increase the temperature respecting the imposed performances, from the value of 1106⁰C (temperature which is being maintained in the first sector of the furnace when, for different reasons, it does not work in service of warming up the billets) to the work value of 1240⁰C. The temperature of 1106⁰C is maintained constant using a constant flow of 85 Nm³/h. These values are considered values 0 for the automatic control system (0⁰C, respectively 0 Nm³/h). In other words, the automatic control system reacts only when the temperature increases over the value of 1106⁰C. If we introduce in the program the parameters that correspond to the first sector, the comparative graph between the numerical and analytical response in the internal centre of the furnace (at 2,5 m distance from both the internal and external wall of the furnace, in the thermocouples) is presented in figure 2:

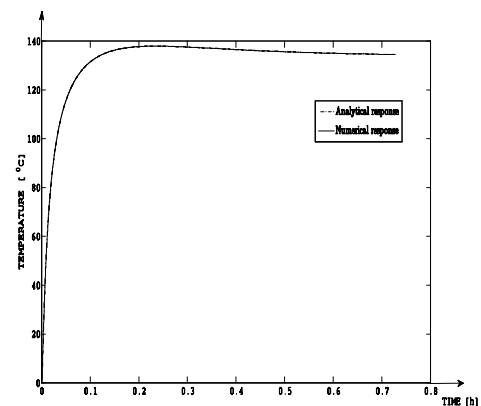


Fig. 2. Analytical response and numerical response of the automatic control system for sector 1.

The temperature reference has been set to the value of 134⁰C (1240⁰C-1106⁰C). In figure 2 it can be noticed that the

system's response in both cases tends asymptotically to the value of 134°C , and then it becomes stable to this value, so the stationary error at the position is $a_{stp}=0^{\circ}\text{C}$. The overshoot is $s = \frac{y_{\max} - y_{st}}{y_{st}} = \frac{137,9 - 134}{134} = 2,9\%$, where

y_{\max} is the maximum value of the response, and y_{st} is the steady state value of the response. In this case the overshoot is much lower than the imposed value of 10%. The overshoot value, as it is situated inside the stationary band of $\pm 3\%$, the system settling time is smaller than the value of the moment when the overshoot occurs. So $t_r = 0,091\text{ h}$, a value that is much lower than the one imposed (0,15h). On the graph we cannot differentiate the two responses due to the very small error between them. The maximum value of the cumulated error in percents in this case is of 0,32%, right at the beginning of the numerical integration, then it falls suddenly and remains constant at the value of $2,82 \cdot 10^{-5} \%$.

Figure 3 presents the execution signal (the input gas flow in the process) obtained through numerical integration:

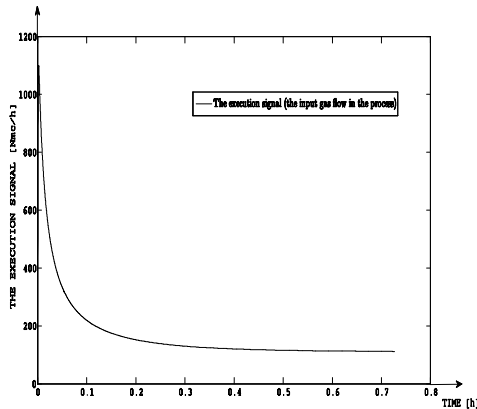


Fig. 3. Simulated execution signal through numerical integration.

Immediately after starting the simulation, when the controller forces the heating of the sector, the maximum value of the gas flow is of $1100,6\text{ Nm}^3/\text{h}$. After the sector temperature gets the reference value, the gas flow value remains constant at $112\text{ Nm}^3/\text{h}$. If we add the existing flow of $85\text{ Nm}^3/\text{h}$, the maximum value of the gas flow becomes $1185,5\text{ Nm}^3/\text{h}$, and its steady state value is $197\text{ Nm}^3/\text{h}$. Comparing the maximum value of $1185,5\text{ Nm}^3/\text{h}$ to the maximum pipe flow of $1290\text{ Nm}^3/\text{h}$, we get the physical possibility to apply this actuation, as it does not get to the saturation level (the maximum pipe flow).

An important aspect in discussing the problem is to introduce the disturbance in the system. In this case the disturbance is represented by the quantity of material (slab billet) that has to be heated. The quantity of material that corresponds to the most unfavourable case (for maximum productivity) is equivalent to the methane gas flow needed to heat this quantity. In the case of the first sector, the value of the

“disturbing” methane gas flow is $D_{p1} = -999,05$

Nm^3/h . The most unfavourable case is featured by a disturbance signal of step type, having the value previously mentioned, that is present in the system when the furnace starts heating to restart the running regime. Theoretically, this situation might occur when, previously, there is a failure in equipment from the technological flow or even at the furnace, and the furnace was completely loaded and was working in parameters of maximum productivity. In this kind of situations, the temperature in the furnace should be reduced, and the hearth should be moved either in only one direction, or alternatively in both directions, according to the specific of the failure. However, the most unfavourable case will not occur because the block will accumulate in the furnace a certain quantity of heat during the failure procedure. On the other hand, the hypothesis that has previously been presented gets very close to it. The simulation will take place considering the disturbance equal to D_{p1} . Figure 4 presents the comparative curve between the analytical response and the numerical response for the automatic control system, to which the disturbance D_{p1} is added. In this situation the stationary deviation to position is 0, the response time has the value $t_{r1} = 0,48\text{h}$ (this high value can be explained through the presence of the material that will absorb a big quantity of heat), and the overshoot does not occur ($s_2 = 0$) because the temperature increase is much reduced by the presence of disturbance. From figure 5 results the maximum value of the execution signal of $1203,4\text{ Nm}^3/\text{h}$ and its stabilization value of $1110,04\text{ Nm}^3/\text{h}$. Considering the initial value of the gas flow of $85\text{ Nm}^3/\text{h}$, the total flow is $1288,4\text{ Nm}^3/\text{h}$, smaller than the saturation flow of $1290\text{ Nm}^3/\text{h}$.

The controller, rejecting the effect of disturbance in the most unfavourable case, can be used for the whole range of disturbances, and the performances will be improved while their value decreases. The relative error cumulated in percentage fluctuates insignificantly from the value point of view comparing with the previous case.

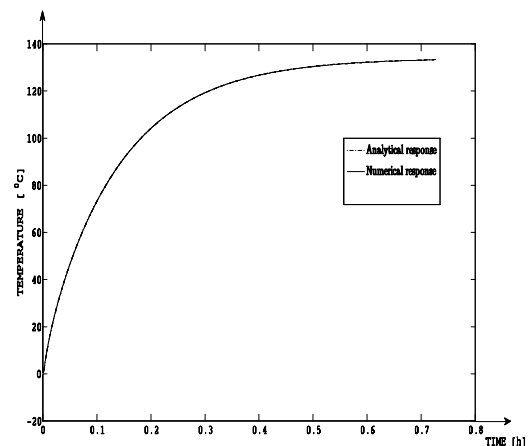


Fig. 4. Comparative curve between the analytical response and the numerical response of the automatic control system for sector 1, when the disturbance is maximum.

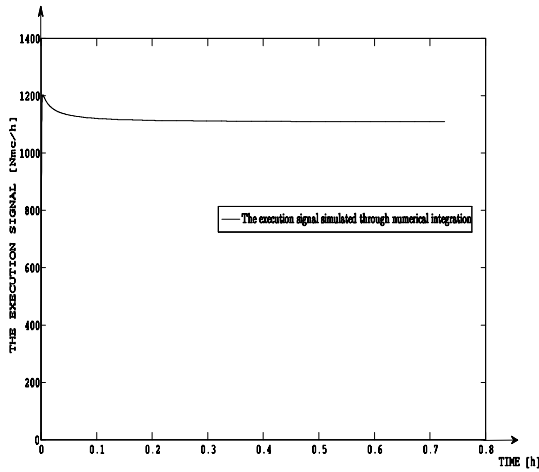


Fig. 5. The execution signal simulated through numerical integration, when the disturbance is maximum.

In figure 6 is presented the evolution of intermediary variables $m_0(t)$, $a_0(t)$ and $c_0(t)$.

A situation that might occur is to apply the disturbance after the dynamic service finishes, meaning after the sector heats without material. The system numerical response in the most unfavorable case (maximum disturbance of step type) is presented in figure 7.

In figure 7 the disturbance occurs at the moment $t=0,363$ h, after the free process (without billets) gets to the steady state.

One can notice that the temperature falls with $38,2^{\circ}\text{C}$ immediately after the disturbance occurs, but it gets back at the imposed value after $0,645\text{h}$, the controller rejecting the disturbance effect. The execution signal (figure 8) does not exceed the maximum rated value of $1290 \text{ Nm}^3/\text{h}$ [8].

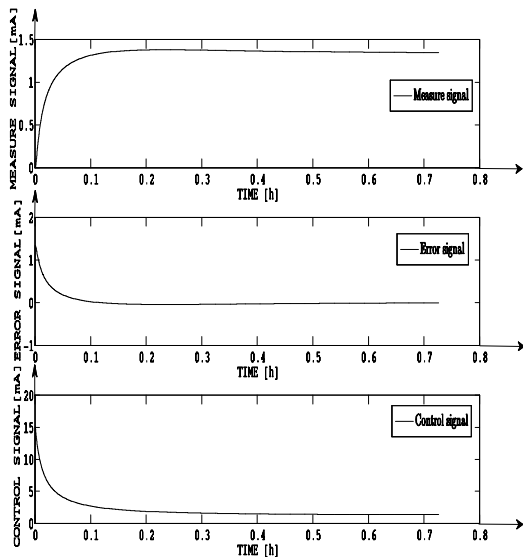


Fig. 6. Evolution of intermediary variables $m_0(t)$, $a_0(t)$ and $c_0(t)$, simulated through numerical integration.

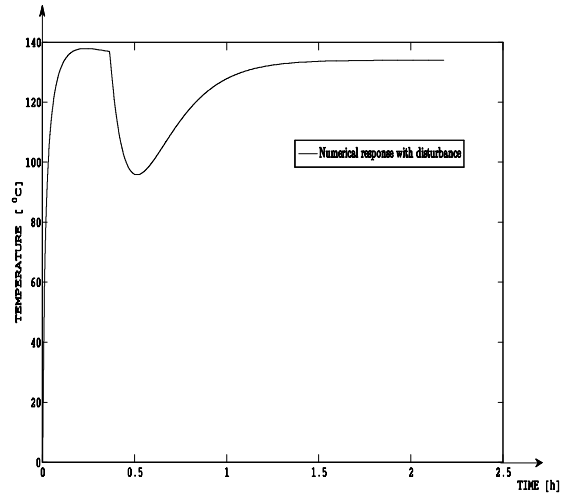


Fig. 7. Numerical response of the automatic control system for sector 1, when the maximum disturbance occurs after the sector is heated.

In figure 9 is presented an extreme case of variation of disturbance, that can occur when in the furnace is exactly the quantity of slab billets that covers only a sector. In this way the slab billet gets slowly in the sector, absorbing more and more heat, gets to the maximum equivalent with D_{p1} , and then leaves the sector slowly, absorbing less and less heat. In this case the disturbance is represented by a negative semi-sine curve that has the formula:

$$SSN = D_{p1} \cdot \sin(w \cdot t), \tag{33}$$

where w - pulsation, t - time, $(w \cdot t) \in (i \cdot p, 2 \cdot i \cdot p)$, and i - natural uneven number and $i > 0$.

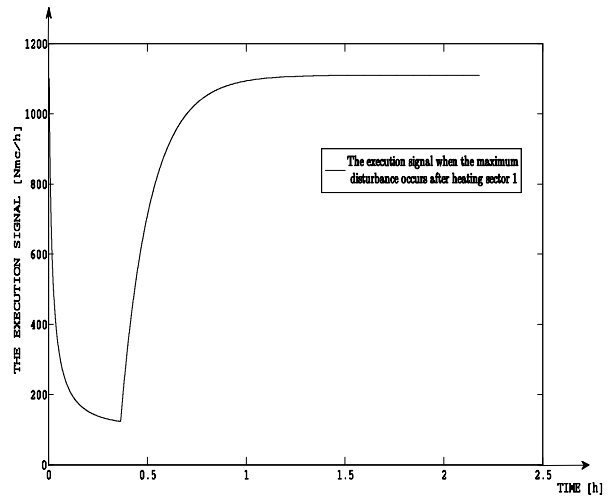


Fig. 8. The execution signal simulated through numerical integration, when the maximum perturbation occurs after heating sector 1.

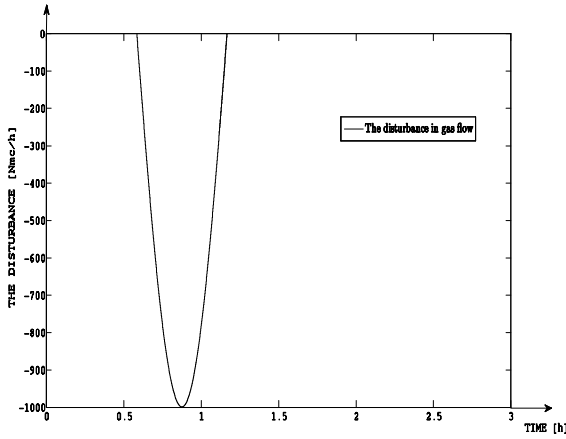


Fig. 9. Disturbance signal of semi-sine form.

The usual complete loading + unloading time of a sector is of almost 0,6 h. The numerical response of the system, when the semi-sine disturbance occurs after the response of the control system gets in steady state, is presented in figure 10.

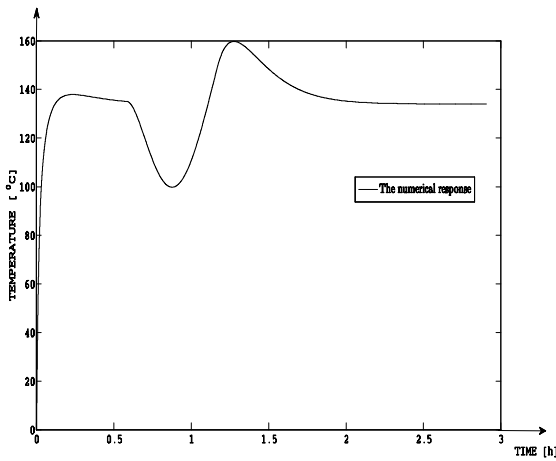


Fig 10. The numerical response of the system, when the semi-sine disturbance occurs after heating sector 1.

The corresponding execution signal, obtained through numerical integration, is presented in figure 11.

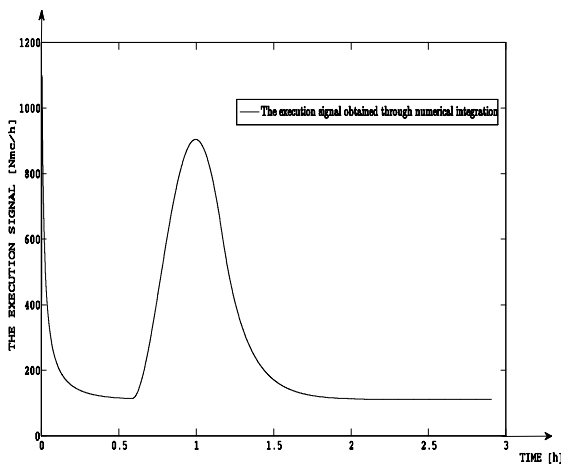


Fig. 11. The execution signal obtained through numerical integration, if the semi-sine disturbance occurs after heating sector 1.

In figure 10 the effect of the disturbance leads to a variation of the response around the steady state value of 134⁰C. In the first stage the temperature decreases with 34⁰C, and in the second stage it increases with 26⁰C over the steady state value, after which the response stabilizes to the reference value. The temperature variation is acceptable although the initial conditions are considered (initial temperature is of 1106⁰C). The settling time is a little longer than in the disturbance of step type case, due to the very fast variation of the disturbance signal. Comparing it with the previous case, the system response does not decrease that much after the disturbance occurs. Also, the maximum value of the execution signal (figure 11) is of 1101 Nm³/h, and if we add the flow of 85 Nm³/h to it (initial conditions referring to flow), implies a smaller value than the saturation value (1290 Nm³/h).

The experimental response and the simulated response of the process (resulted from the experimental identification procedure), for sector one, are presented in figure 12.

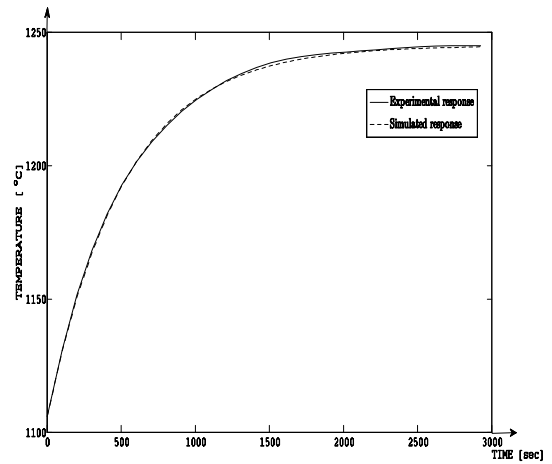


Fig. 12. Comparative graph between the experimental step response and the simulated step response of the process for sector one.

6. CONCLUSIONS

1. This paper presents the method of analogue modeling and numerical simulation of the automatic control system of the temperature value in the furnace with rotary hearth.
2. The simulation results obtained after the implementation of the method have been presented, corresponding to the first sector of the furnace.
3. The automatic control scheme can be used both to control the billet temperature and to control the temperature of the gases in the work area (the external space to the billet – the version that is preferred and which is presented in this paper).
4. The method of numerical control that is used is a general one, the user having access to the values of all the intermediate variables. In order to check the performances of numerical integration we used as comparison standard the

analytical model of the process. In both cases that were studied the performances were very good and the cumulated relative error in percents as very small values.

5. Using the equations with partial derivatives allows a presentation that is very close to reality of the way the 5 thermal processes work. The case of modeling through transfer functions is a particular case of modeling through equations with partial derivatives.

6. In order to calculate the controllers we've adapted the module method to the partial derivatives equations. Thus the obtained performances do not agree completely to the module criterion. All the imposed performances have been respected.

The authors express their thanks to Professor Tiberiu Colosi, for his help in elaborating this work.

REFERENCES

Different technical papers of Tenaris Silcotub Zalău.

- I. Pența, D. Szeredai, F. Major, "The technology of preparing the loading of the CVR and perforating the blocks in the Mannesmann perforator", Bucharest, 1987.
- M. Abrudean, „Systems theory and automatic regulation“, MEDIAMIRA Publishing house Cluj-Napoca, 1998, 170 pag.

Tiberiu Coloși, Mihail Abrudean, Eva Dulf, Mihaela-Ligia Ungureșan, "Numerical Modelling and Simulation Method for Lumped and Distributed Parameters Processes with Taylor Series and Local Iterative Linearization", Cluj-Napoca 2008.

Tiberiu Coloși, Mihaela-Ligia Ungureșan, Eva Dulf, Roxana Carmen Cordoș, "Introduction to Analogue Modeling and Numerical Simulation with (M) and Taylor Series Distributed Parameters Processes", GALAXIA GUTENBERG Publishing house, Cluj-Napoca, 2009.

User Guide, Matlab 7.5.0 (R2007b).

Vlad Mureșan, Mihail Abrudean, 2008 IEEE International Conference on Automation, Quality and Testing, Robotics Proceedings-TomeII, "The control of the step for the furnace with rotary hearth in the technologic flow for manufacturing pipes without welding", ISBN:978-1-4244-2576-1, pp.258-266.

Vlad Mureșan, Mihail Abrudean, "Experimental identification and numerical simulation of thermal processes associated with the furnace with rotary hearth", ACAM, vol. 18(2009), No. 1, pp. 31-43, ISSN: 1221-437X.